PARAMETRIC STUDIES OF STITCHING EFFECTIVENESS FOR PREVENTING SUBSTRUCTURE DISBOND

Gerry Flanagan
Materials Sciences Corporation
Fort Washington, PA

Keith Furrow
Lockheed Engineering & Sciences Co.
Hampton, VA

INTRODUCTION

A methodology is desired that will allow a designer to select appropriate amounts of through-thickness reinforcement needed to meet design requirements. The goal is to use a relatively simple analysis to minimize the amount of testing that needs to be performed, and to make test results from simple configurations applicable to more general structures. Using this methodology, one should be able to optimize the selection of stitching materials, the weight of the yarn, and the stitching density.

The analysis approach is to treat substructure disbond as a crack propagation problem. In this approach, the stitches have little influence until a delamination begins to grow. Once the delamination reaches, or extends beyond a stitch, the stitch serves to reduce the strain-energy-release-rate (G) at the crack tip for a given applied load. The reduced G can then be compared to the unstitched material toughness to predict the load required to further extend the crack. The current model treats the stitch as a simple spring which responds to displacements in the vertical (through-thickness) direction. In concept, this approach is similar to that proposed by other authors. See Ref. 1 for example. Test results indicate that the model should be refined to include the shearing stiffness of the stitch.

The strain-energy-release-rate calculations are performed using a code which uses interconnected higher-order plates to model built-up composite cross-sections. When plates are stacked vertically, the interfacial tractions between the plates can be computed. The plate differential equations are solved in closed-form. The code, called SUBLAM, was developed as part of this

section in one dimension. Because of this limitation, rows of stitches are treated as a two-dimensional sheet. The spring stiffness of a row of stitches can be estimated from the stitch material, weight, and density. One unknown in the analysis is the effective length of the spring, which depends on whether the stitch is bonded to the surrounding material. This issue was examined in Ref. 4. As a practical and conservative approach, we can assume that the stitch is bonded until a crack passes the stitch location. After the crack passes, it is fully debonded.

A series of tests were performed to exercise the methodology outlined above. The test incorporated an attached flange such that the sudden change in thickness initiated a delamination. Two load conditions were used (3-point and 4-point bending) so that ratio of shear load to moment load could be varied. The analysis was used to estimate the material's critical G from the unstitched specimens. With this data, a prediction was made for the load required to delaminate the stitched specimens.

Using the methodology, design charts have been created for simplified geometries. These charts give stitch force, along with G_I and G_{II} as a function of the stitch spring stiffness. Using the charts, it should be possible to determine the stitch spring stiffness and strength required to reduce the G to a desired level. From these parameters, the actual stitching material, weight, and density can be computed. The results have been nondimensionalized for wider applicability.

VERIFICATION TEST

Specimen Fabrication

The two test specimen configurations are shown in Fig. 1. The specimens were fabricated from dry, AS4 uniweave fabric preforms that were resin film infusion molded (RFI) with 3501-6 resin. Uniweave fabric consists of unidirectional Hercules AS4 carbon fiber tows woven together with 225 denier glass fibers. The weave fibers made up a small portion (~2%) of the weight of the fabric. Each configuration had a stitched and unstitched version.

The stitched flanges were attached to the skin before molding by laying up the skin and flange together and mounting them in a 34 inch by 34 inch sewing frame. Then 4 inch or 2 inch wide rows of 1600d Kevlar 29 lock stitching secured the flanges to the skin. The stitch rows were 0.2 inches apart , with a 0.125 inch step. After stitching, the excess flange material was cut away.

During the RFI process, the dry textile preforms were placed on top of a pre weighed film of degassed 3501-6 epoxy resin lying in the bottom of the metal mold. The mold cover had a cavity in the shape of the flange. Holes vented the excess resin. After closing the mold and sealing it around the edges, the entire mold was placed in a hot press and evacuated at 30 mm Hg. Platens at 285°F heated the preform to reduce the viscosity of the resin and mechanical pressure (100 psi) from the platens forced the resin into the fabric preform. Raising the platen temperatures to 350°F and holding for 2 hours fully cured the composite panels.

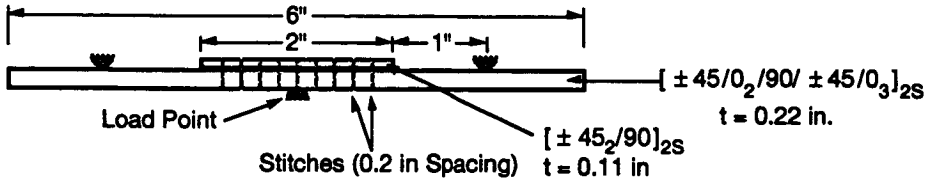

Figure 1. Three-point bending specimen with stitched attached flange.

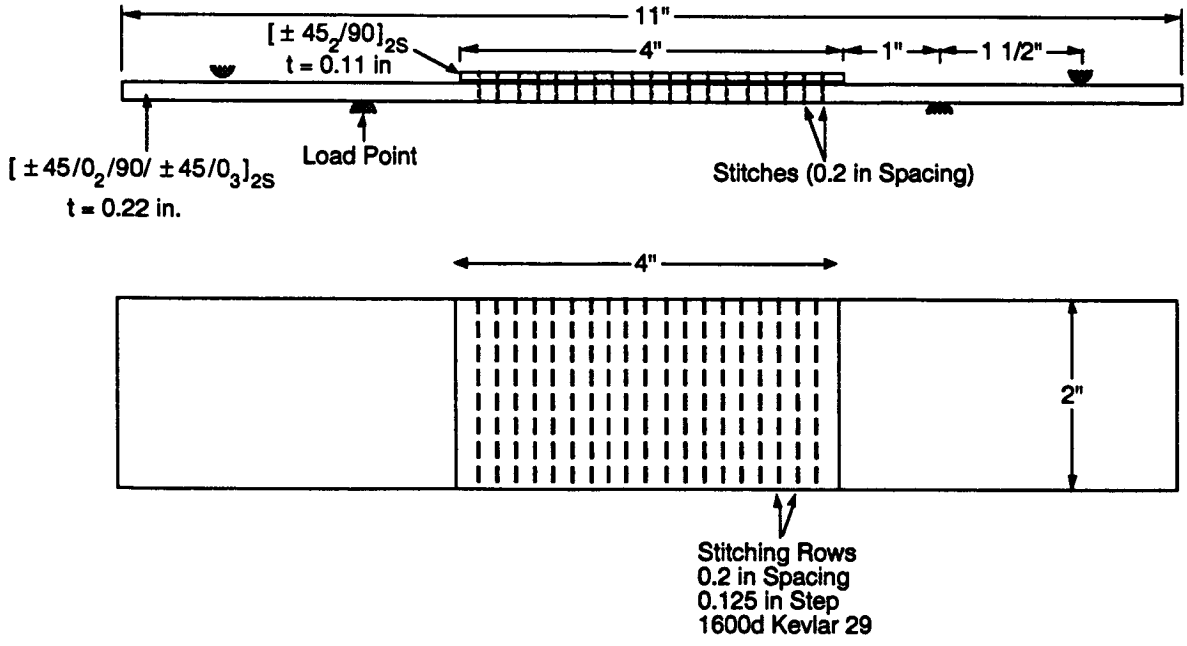

Figure 2. Four-point bending specimen with stitched attached flange.

The fiber volume fractions were 58 to 59 percent. C-Scans of the panels showed very few voids, however, a resin rich area on one side of the flange and bent or displaced fibers on the other

side of the flange were visible on some of the unstitched panels. The flange shifting after closing the mold potentially caused this problem.

Test Procedure

A crosshead rate of 0.02 inches per minute loaded the bending specimens while the load, displacement and crack growth were monitored. The load cell on the hydraulic load frame measured the load and a displacement transducer measured the center span displacement. The edges of the specimens were painted with white paint to make the crack clearly visible. A rule with 0.1 inch spacing was drawn on the side of the specimen to record the crack length as a function of the load. The crack length and load were manually recorded nominally every 0.1 inches of crack length . When the crack reached the center of the specimen the 3-point bend test was stopped. The 4-point bend test was stopped after a crack propagated one inch. The tests did not use any form of starter crack.

Results

A typical pair of load-displacement curves are shown in Fig. 3 for stitched and unstitched 3-point bending specimens. The sudden discontinuities in the curves correspond to sudden extensions of the crack. The curves also show that the stitched specimen is stiffer than the unstitched, beginning with the initial linear portion of the curve. The average stiffness for the stitched 3-point specimens was 15% greater than for the unstitched specimens, while the stitched 4-point specimens were 9% stiffer than the corresponding unstitched version. Using properties for AS4/3501-6 Uniweave taken from Ref. 5, the stiffness was calculated using both finite elements and SUBLAM. The calculated values were 9% and 7% greater than the experimental values for the 3-point and 4-point stitched specimens, respectively. The analysis requires the interlaminar shear stiffnesses, G_{13} and G_{23}. These values were not available, and therefore typical Gr/Ep values (G_{13} = 0.8 Msi, G_{23} = 0.5 Msi) were used in the original analysis. One hypothesis for the discrepancies in stiffness is that the actual transverse shear stiffnesses of this material are less than the assumed values, perhaps due to the uniweave form. Consequently, the values in the analysis were adjusted downward (G_{13} = 0.4 Msi, G_{23} = 0.25 Msi) to obtain a better correspondence between the test and analysis.

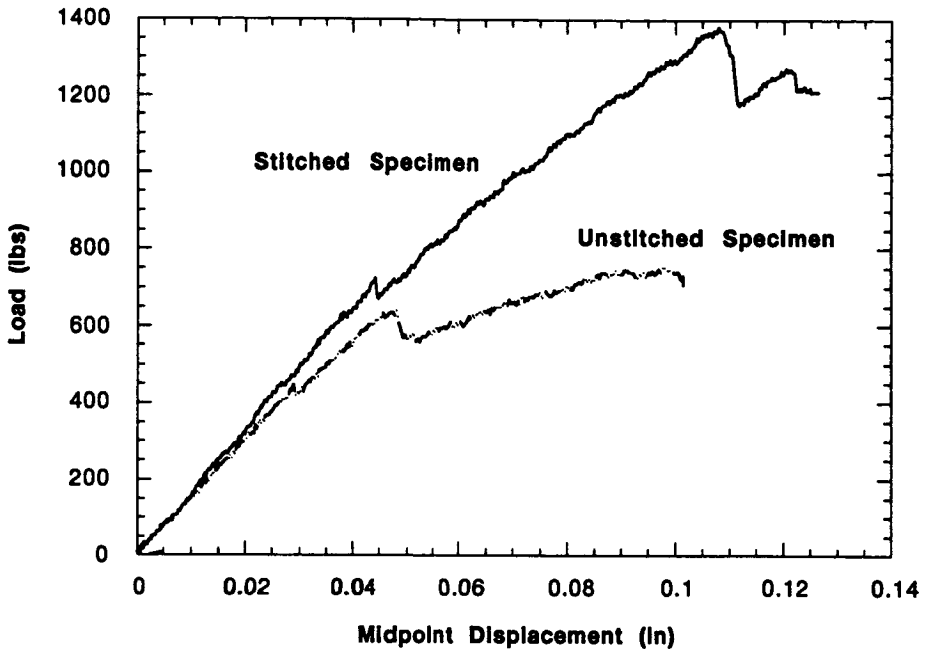

Figure 3. Typical force-displacement curves for stitched and unstitched 3-point bending specimens

From the load versus crack length data for the unstitched specimens, the strain-energy-release-rate can be back-calculated. The results of this calculation are shown in Fig. 4 for the mode I and mode II components. In these plots, "a" is the crack length. Ideally, the values obtained from the 3-point and 4-point specimens should overlap. However, the results show that the 3-point specimens tend to have a lower value of G. The plots also indicate that G increases with crack length. The increase in G with the crack length is frequently associated with bridging of fibers. The initial G_I is greater than would normally be expected for 3501-6 resin. This may be due to the lack of a starter crack, or to the uniweave material form. Finally, we note that the 4-point specimens number 4 and 5 appear to be outliers, although there was no obvious difference in these specimens.

The stitching analysis requires both the critical G_I and G_{II} ($G_{Icrit}$and G_{IIcrit}). The unstitched specimens are mixed-mode, but do not provide sufficient information to determine both values. Based on typical Gr/Ep properties, we assumed that $G_{IIcrit} = 4\ G_{Icrit}$. The following linear mixed mode crack growth criteria was also assumed.

$$\frac{G_I}{G_{Icrit}} + \frac{G_{II}}{G_{IIcrit}} = 1$$

Using these two assumptions, G_{Icrit} was determined so that a good fit to the initial crack extension load for the unstitched specimens was obtained. This yielded a G_{Icrit} of 2.2 in-lb/in^2.

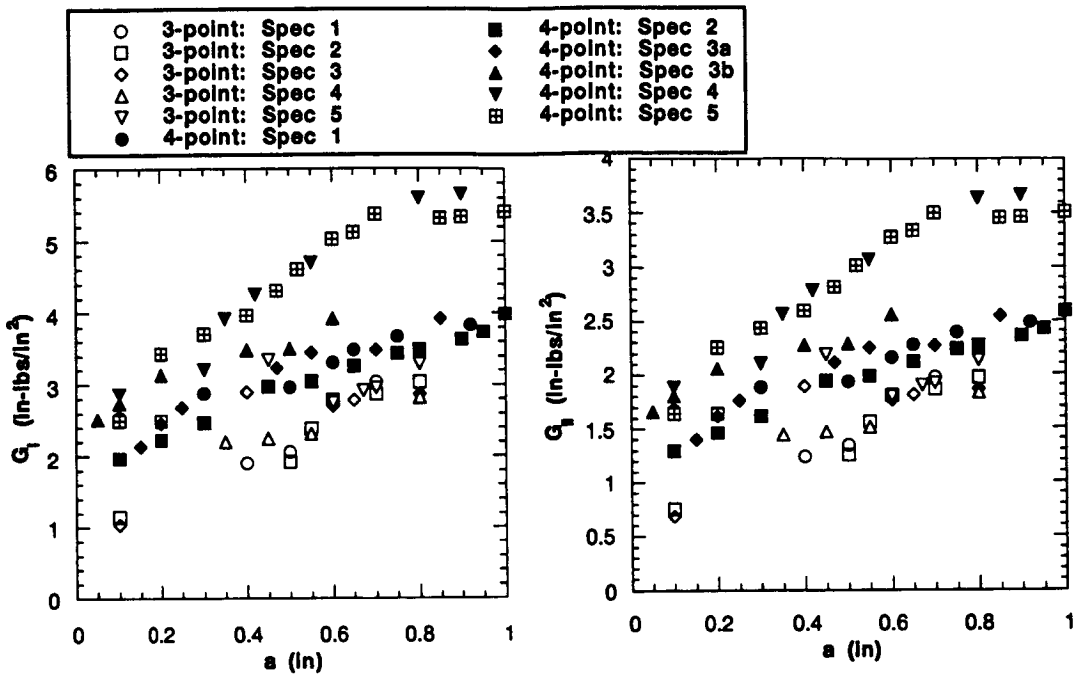

Figure 4. Experimental values of G_I and G_{II} versus crack length.

The predicted and experimental loads for crack growth are given in Fig. 5 and 6. Two values of the stitched spring stiffness were used. The first, $k=1.2 \times 10^5$ lb/in^2, assumes that the stitch is fully debonded. The second, $k = 4.7 \times 10^5$ lb/in^2, assumes that the stitch is bonded, but that the matrix behaves as an elastic-plastic material, calculated using the methods given in Ref. 4. Both curves for the stitched cases fall below the experimental data. The change in assumed stitch stiffness affects how rapidly the stitches begin to suppress the crack growth, but has little effect on the maximum load that may be applied. The predictions use the initial values of G, and do not take the observed crack resistance curve into account. Therefore, in Fig. 5, the unstitched predicted load goes down with increasing crack length (unstable growth), while the experimental values increase with crack length.

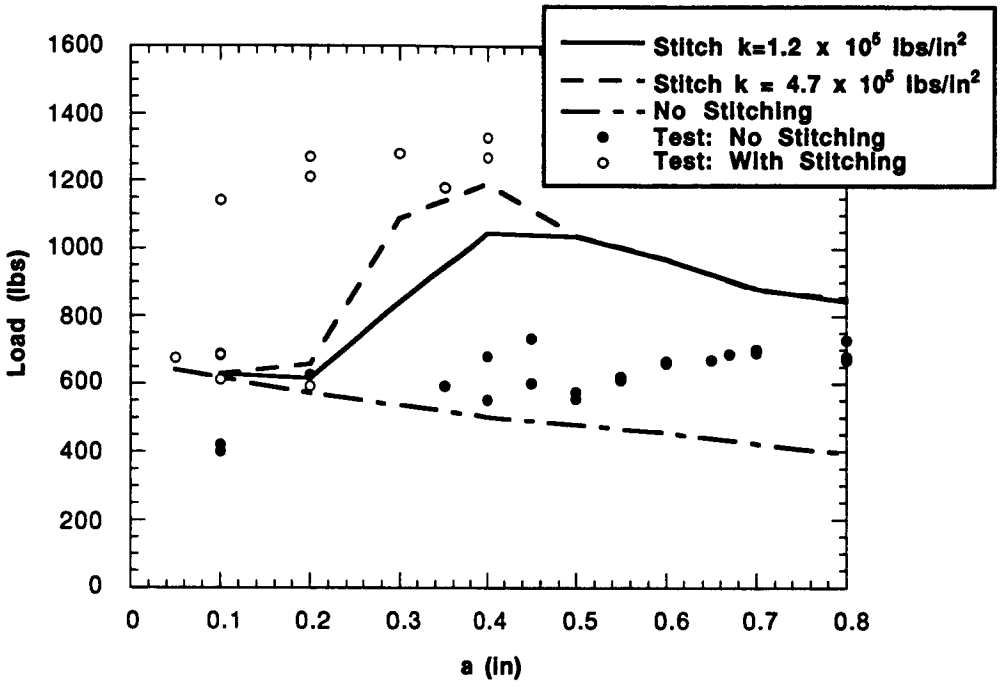

Figure 5. Predicted and measured loads required for crack extension. Three-point bending case.

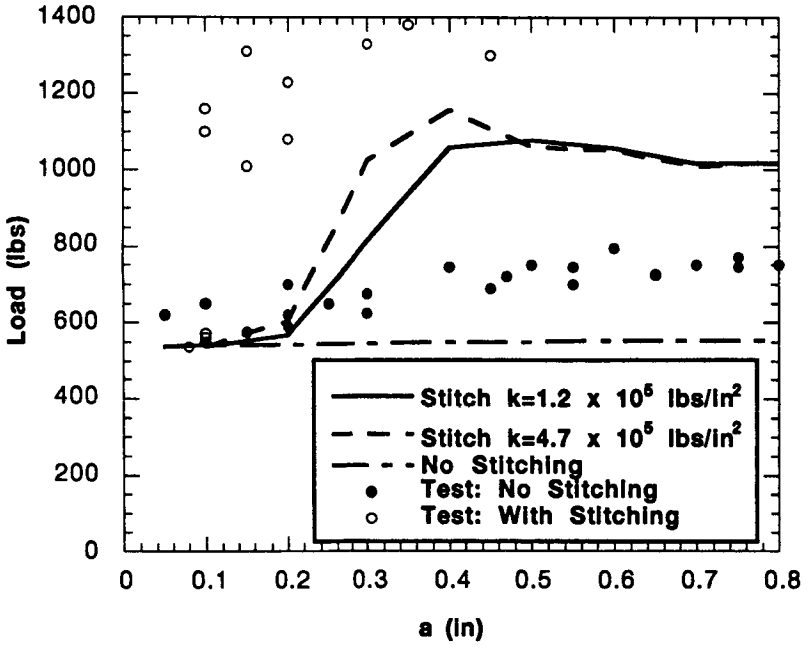

Figure 6. Predicted and measured loads required for crack extension. Four-point bending case.

The failure of the analysis to predict the full effect of the stitches may be related to the simple model in which the stitch only resists through-thickness stretching. In this model, the stitch does nothing to suppress mode II crack growth. In the analysis of the stitched specimens, the stitching was sufficiently stiff to completely suppress mode I crack growth. The results indicate that stitches also reduce mode II growth. Fig. 7 shows the sliding displacement that occurs at the stitch locations in the 3-point bending specimens. Stitches may resist this sliding motion either by shearing, or by local large rotations.

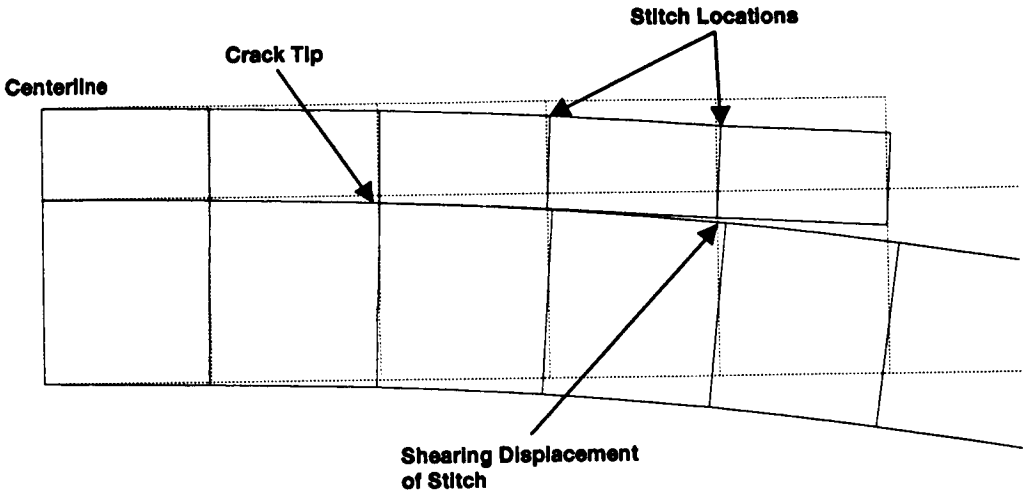

Figure 7. Deformed three-point bending specimen from SUBLAM analysis

PARAMETRIC STUDIES

The inherent design flexibility of composite structures makes it difficult to create generic design graphs. Consequently, design with composite invariably involves computer software. However, some highly idealized configurations can be treated in a parametric manner to give a feel for the mechanics involved, and to give order-of-magnitude estimates for the stitch parameters needed to stop delamination growth. Such idealizations have been examined using the SUBLAM program in order to create a series of design charts.

A number of simplifications had to be made to create problems that can be nondimensionalized. One simplification is that we treat plates made from a homogeneous, orthotropic material, instead of laminates. This removes stacking sequence considerations from the problem. For the problems

studied, we have further assumed the orthotropic material has the properties of a quasi-isotropic layup of graphite/epoxy.

Another simplification involves our treatment of delamination growth. A general analysis would involve tracking the growth of a delamination until either unstable growth occurs, or the structure collapses. The simplified approach is to determine the strain-energy-release rate for a delamination of a predetermined size. Furthermore, we assume the delamination size is smaller than the spacing between stitches. Thus, the models include only a single row of stitches. The approach being presented implies that the through-thickness reinforcement should be selected to stop a delamination within a single row of stitches; a conservative criterion.

The stiffness of the stitch is an independent parameter in the design charts. Our models assume that the cross-section of the structure is constant. Consequently, a row of stitches is actually treated as a 2-dimensional sheet. The spring stiffness, k, of such a sheet is defined by the force-displacement relation

$$k = N/\delta$$

where δ is the displacement, and N is a running load with units lb/in. Therefore, the units of k are lb/in^2, and k can be estimated by the relation

$$k = 6.222 \times 10^{-9} \frac{E\, n\, w}{\rho\, l} \quad lb/in^2$$

where E is the modulus of the stitching material (lb/in^2), n is the stitch pitch along the row (penetrations/in), w is the weight of the stitch in Denier, ρ is the volume density of the stitch material (lb/in^3), and l is the effective length of the stitch (in). The constant represents a unit conversion from Denier to lb/in. A lower bound on the stiffness can be determined by assuming the stitch is fully debonded. In which case, l is the total thickness of the laminate. If the stitch does not fully debond, the effective length is smaller, and the stitch acts as a stiffer spring.

The design charts give running load, f_S (lb/in), for the row of stitches. This load can be used to estimate the applied load needed to fail the row of stitches. The strength of the row can be estimated from

$$f_s^{ult} = 6.222 \times 10^{-9} \frac{\sigma_s^{ult}\, n\, w}{\rho} \quad lbs/in$$

where σ_s^{ult} is the ultimate strength of the stitching material.

The delamination growth criterion used in our charts is the strain-energy-release-rate (G). The charts give the mode I and II values for G. If G_I and G_{II} are determined for a trial applied load, then, assuming a linear interaction curve, the critical load for delamination growth is given by

$$R = \left(\frac{G_I}{G_{I\,crit}} + \frac{G_{II}}{G_{II\,crit}} \right)^{-1/2}$$

where $G_{I\,crit}$ and $G_{II\,crit}$ are the critical material values for pure mode I and mode II, and R is a scaling factor that multiples the trial applied load (assuming proportional loading). In the design charts, the values of G are given in nondimensional form. The combination of parameters used for nondimensionalization are given on the individual charts.

The first idealized geometry treats a sudden change in thickness for a cantilevered beam (Fig. 8). This problem could represent the attached flange of a stiffener. We have assumed that the initial delamination length is $1.25\ h_1$.

Three load cases can be considered; pure moment, pure normal shear at the crack tip, and axial load. The results for the pure moment case are given in Fig. 9-11 for a range of h_2/h_1 values. If one observes the trends with respect to changes in h_2, there appears to be a sudden change in behavior when $h_2 = 0.2\ h_1$. This jump in the results is being investigated. Note that G_{II} actually increases with increasing stitch stiffness. However, for most brittle composites, the critical mode II toughness for the material is much greater than the mode I value. Therefore, the decrease in G_I is more significant toward suppressing delamination.

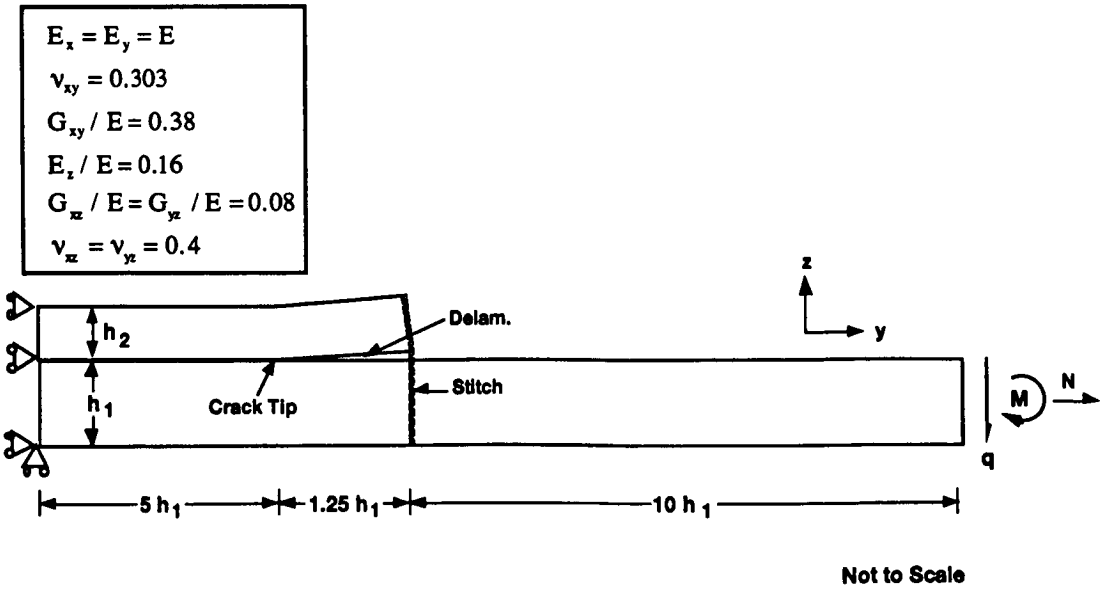

Figure 8. Idealization of attached flange.

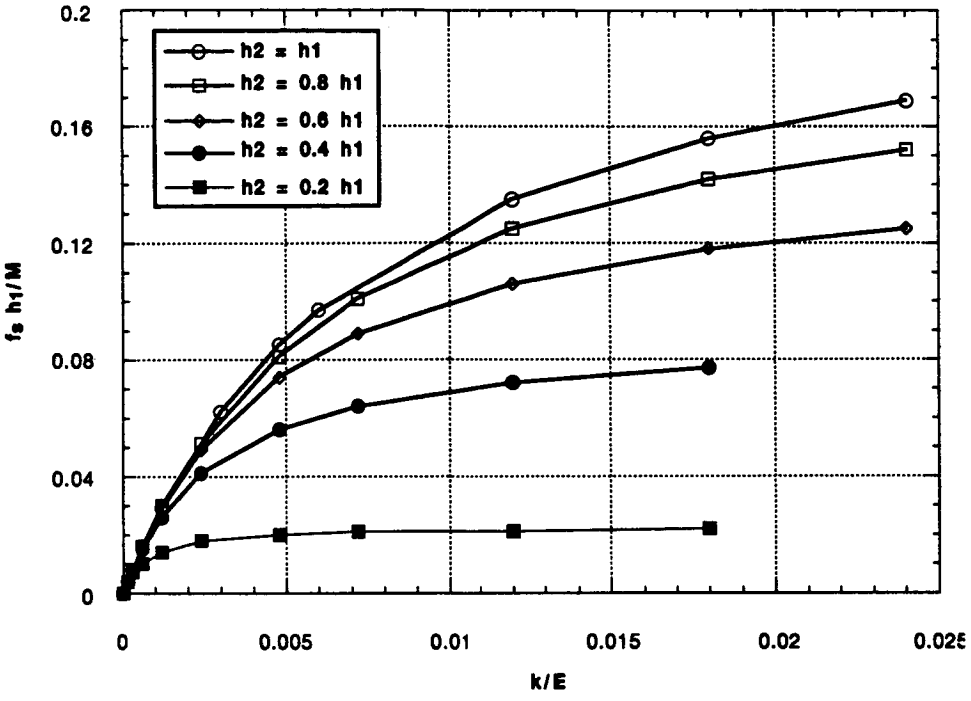

Figure 9. Normalized stitch force for attached flange under moment load.

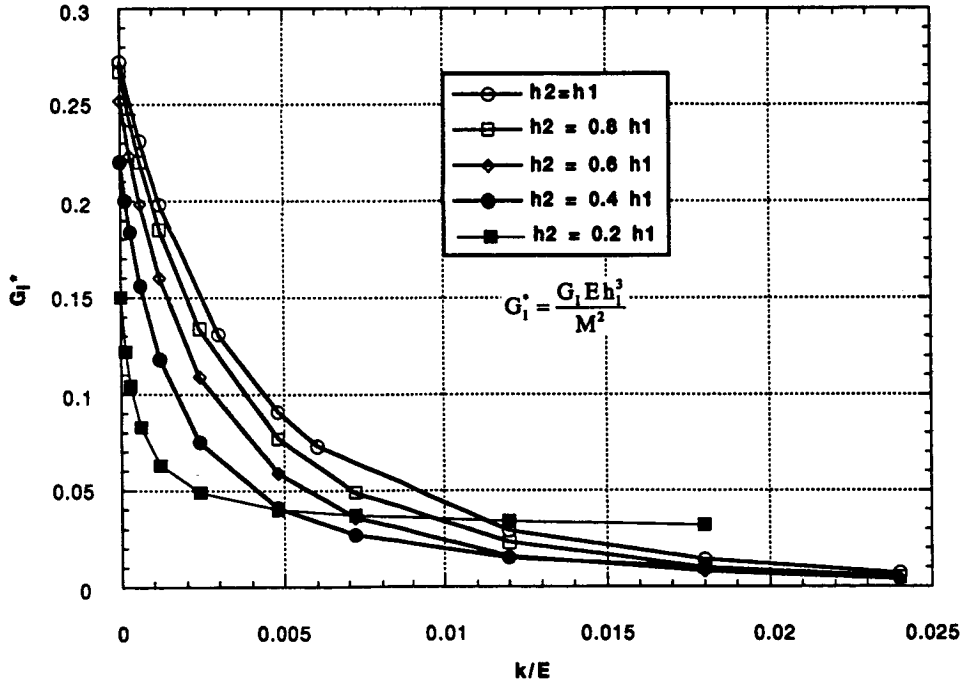

Figure 10. Normalized G_I for attached flange under moment load.

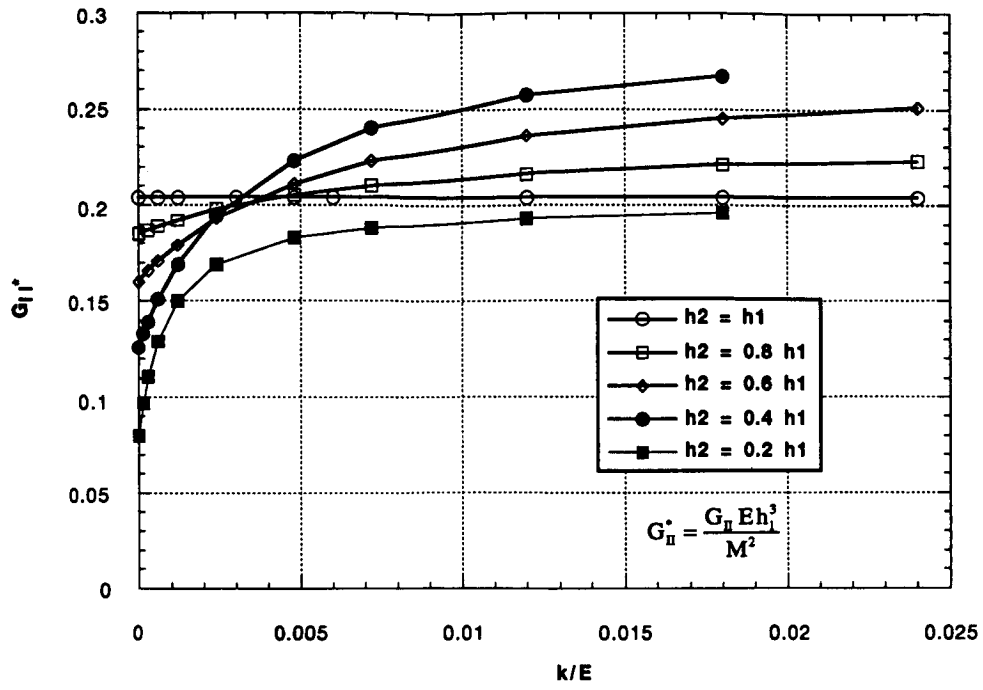

Figure 11. Normalized G_{II} for attached flange under moment load.

To use the charts of this form, it is suggested that the analyst determine the combination of moment, shear and axial load at the crack tip for a particular case. The values of G can be determined from the charts for each load component independently. The individual G's can then be summed, and the interaction equation given above used to determine the load scaling factor (if R is less than 1, then there is a negative margin-of-safety for crack growth). Flanges with gradual tapers can be approximately analyzed by using the local thickness at the stitch row location.

A second idealized problem represents the stiffener pull-off problem (Fig. 12). In this model, we assume that the filler material has already failed. Because the load condition is symmetric, only half of the geometry is modeled, and symmetry boundary conditions are applied. The stitch row is placed at the dividing line between the flat and curved parts of the stiffener laminate. Creating a generic series of plots for this problem is more difficult since the structure is not statically determinant. Thus, the loads at the crack-tip will be affected by the length of the skin segment, and the boundary conditions for the skin. For the idealization, we assume that the skin is clamped at a distance of 50 h_1 from the centerline. The sensitivity of the results to these arbitrary dimensions needs to be investigated. Based on Grumman design practice, the inside radius of the curved laminate is equal to the laminate thickness.

The results for the pull-off problem are given in Fig. 13-15. Curves are not given for $h_2 = h_1$ and $h_2 = 0.8\ h_1$ because the crack was closed for these values, making the stitch ineffective. In these cases, the crack could extend in pure mode II. This behavior may be related to the qualitative observation made in Ref. 6 that stitches placed near the heel of a stiffener appeared to be failing in shear. Figure 14 indicates that G_I approaches a constant value even for large values of the stitch stiffness. Thus, for the assumed delamination length, there is a limit to how effectively the stitches can suppress mode I fracture.

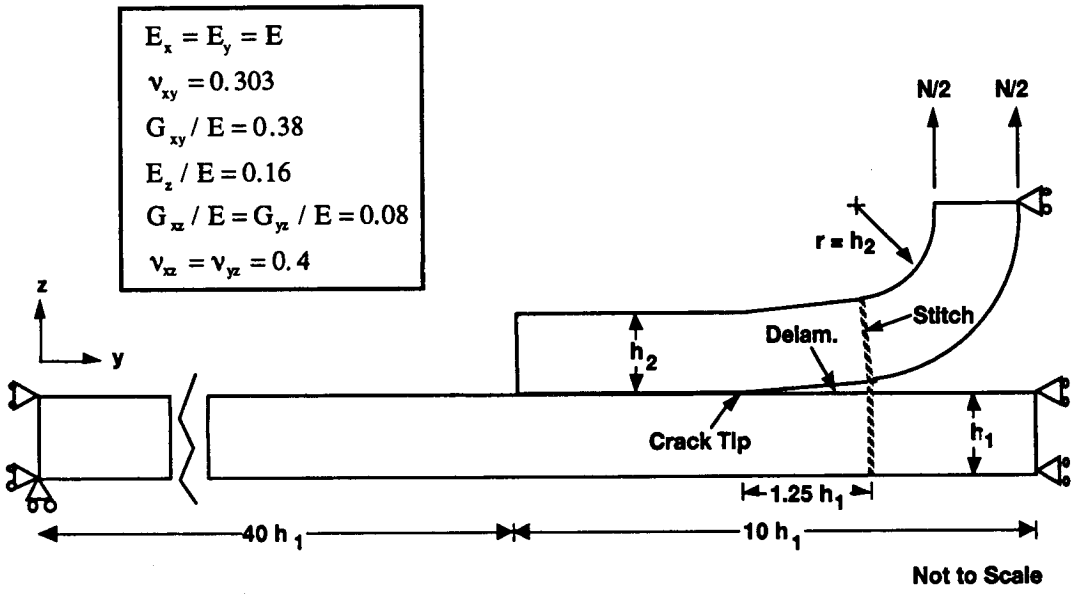

Figure 12. Idealization for stiffener pull-off problem.

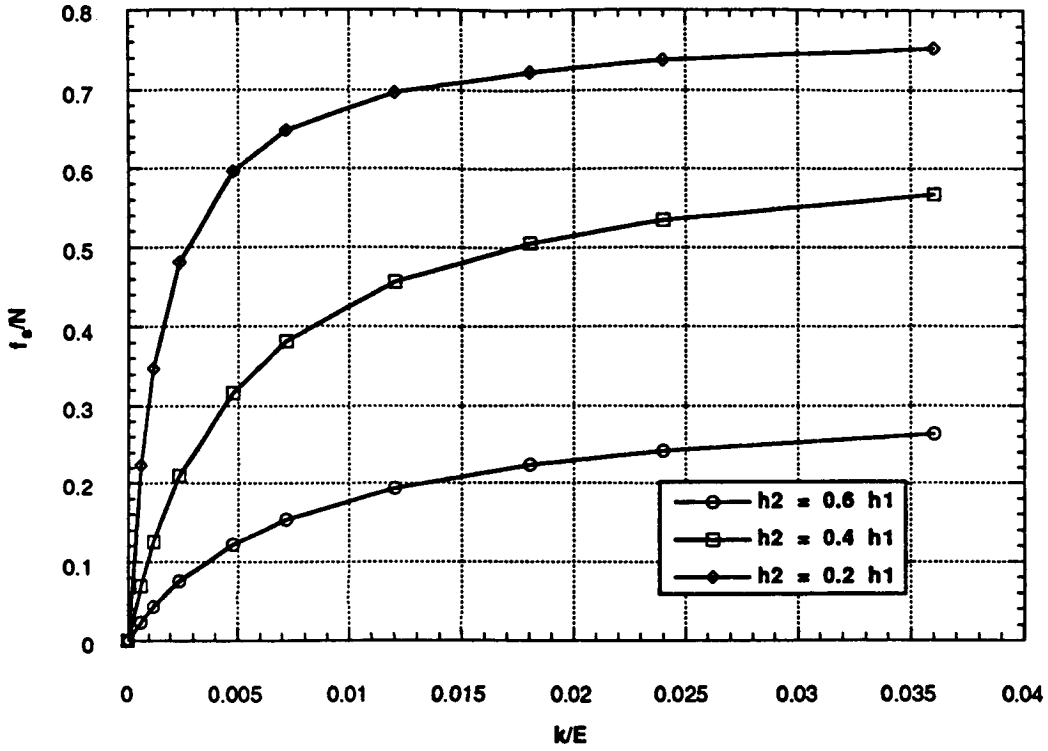

Figure 13. Normalized stitch force for pull-off problem

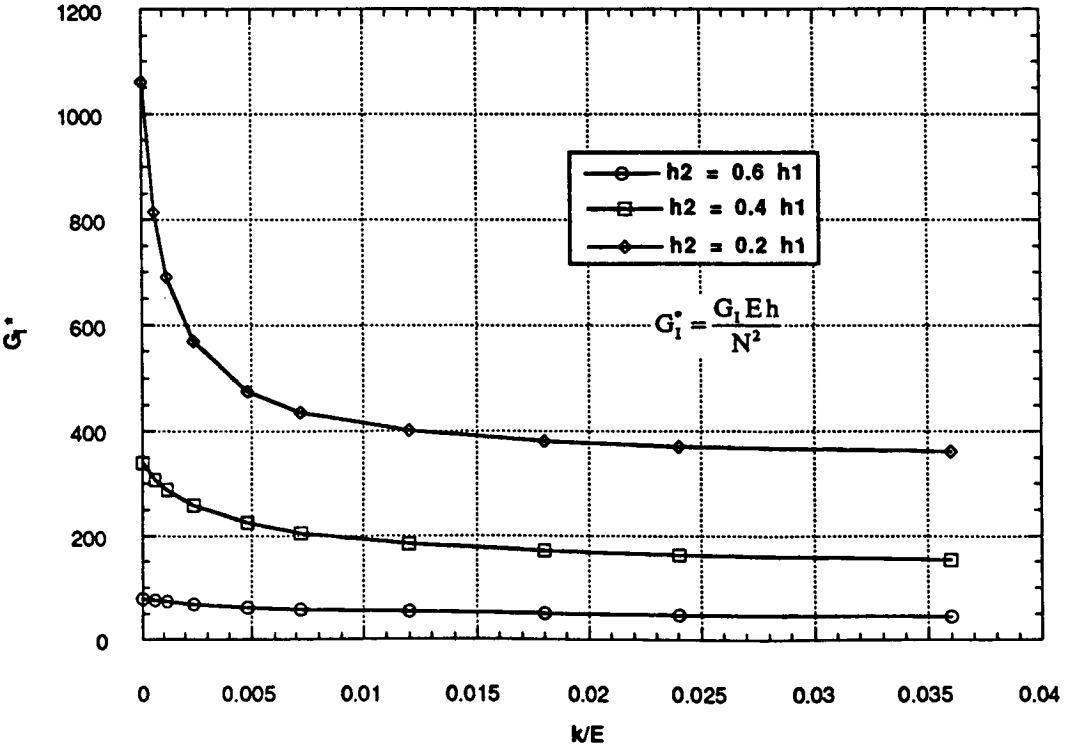

Figure 14. Normalized G_I for pull-off problem

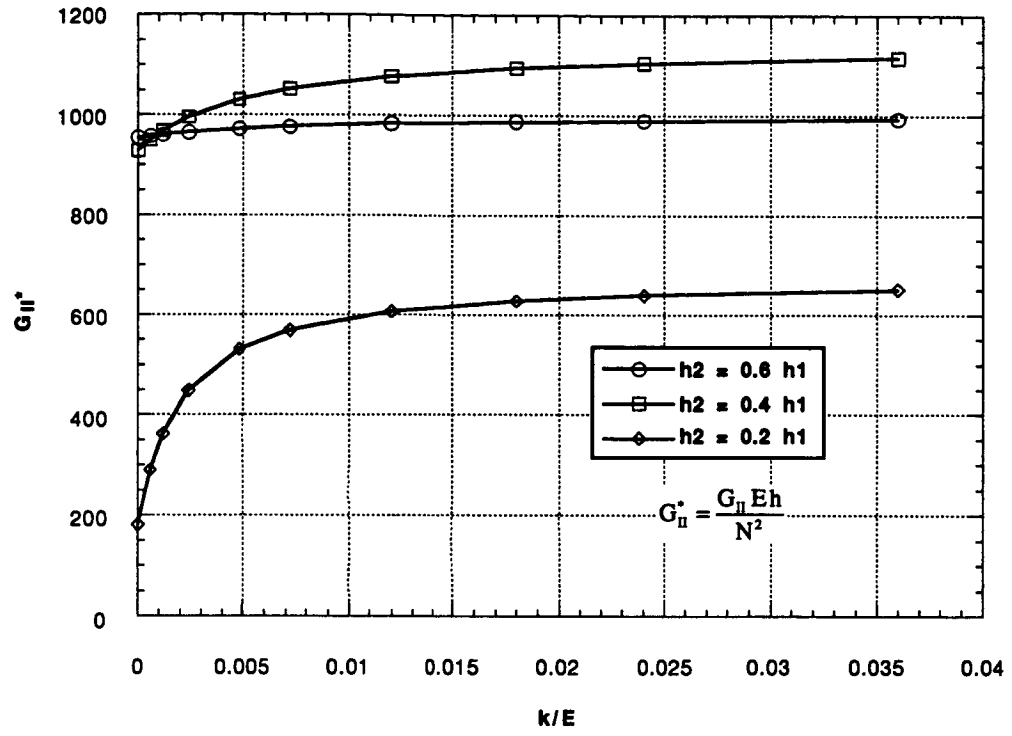

Figure 15. Normalized G_{II} for pull-off problem.

CONCLUSIONS

A methodology has been developed that can be used to select appropriate through-thickness reinforcements. Verification tests of the analysis were somewhat ambiguous because the pure mode I and II fracture toughnesses for the material were not available. The analysis gives conservative results for the amount of additional load a stitched flange can take without delaminating. This conservatism seems to be related to the ability of stitching to suppress mode II fracture, in addition to the mode I behavior included in the model.

The analysis gives us the ability to create non-dimensional curves that help in designing cocured structures with through-thickness reinforcements. Despite the shortcomings revealed in the testing, the analysis provides a conservative method of design, while minimizing the amount of element testing that must be performed.

ACKNOWLEDGMENTS

This work was performed under NASA's Novel Composites for Wing and Fuselage Applications (NCWFA) program, contract No. NAS1-18784, with Mr. H. Benson Dexter as the Contracting Officer Technical Representative. The test specimens were fabricated and tested at NASA/LaRC.

REFERENCES

1. Joon-Hyung Byun, John W. Gillespie, Jr., and Tsu-Wei Chou, "Mode I Delamination of a Three-Dimensional Fabric Composite," J. of Composite Materials, Vol. 24, May 1990, pp 497-518.

2. G. Flanagan, "A Sublaminate Analysis Method for Predicting Disbond and Delamination Loads in Composite Structures," J. of Reinforced Plastics and Composites, Vol. 12, August 1993, pp 876-887.

3. G. Flanagan, "A General Sublaminate Analysis Method for Determining Strain Energy Release Rates in Composites," AIAA Paper 94-1358, 35th AIAA/ASME/ASCE/AHS/ASC Structures, Structural Dynamics, and Materials Conference, Hilton Head, SC, April 18-20, 1994, pp 381-389.

4. G. Flanagan, "Development of Design Guidelines for Stitching Skins to Substructure," presented at the Fourth NASA/DoD Advanced Composites Technology Conference, Salt Lake City, Ut., June 7-11, 1993.

5. "Innovative Composite Aircraft Primary Structures (ICAPS), February 1992 Technical Progress Report," preparted for NASA Langley Research Center under contract NAS1-18862, McDonnell Douglas Corp., pg. 17.

6. C. Cacho-Negrete, "Integral Composite Skin and Spar (ICSS) Study Program - Vol, 1," AFWAL-TR-82-3053, Sept. 1982, pg 269.